Molecular Therapy
Original Article

Chemotherapy-Induced Long Non-coding RNA 1 Promotes Metastasis and Chemo-Resistance of TSCC via the Wnt/β-Catenin Signaling Pathway

Zhaoyu Lin,[1,2,7] Lijuan Sun,[1,6,7] Shule Xie,[1,7] Shanyi Zhang,[1] Song Fan,[1,2] Qunxing Li,[1,2] Weixiong Chen,[1,2] Guokai Pan,[1,2] Weiwei Wang,[3] Bin Weng,[4] Zhang Zhang,[5] Bodu Liu,[1,6] and Jinsong Li[1,2]

[1]Guangdong Provincial Key Laboratory of Malignant Tumor Epigenetics and Gene Regulation, Sun Yat-sen Memorial Hospital, Sun Yat-sen University, Guangzhou 510120, China; [2]Department of Oral & Maxillofacial Surgery, Sun Yat-sen Memorial Hospital, Sun Yat-sen University, Guangzhou 510120, China; [3]Department of Stomatology, Zibo Center Hospital, Zi Bo 255001, China; [4]Department of Pathology, The Affiliated Hospital of North Sichuan Medical College, Nanchong 637600, China; [5]Department of Pathology, West China Hospital, Sichuan University, Chengdu 610041, China; [6]Cold Spring Harbor Laboratory, Cold Spring Harbor, NY 11724, USA

Increasing evidence has shown that chemo-resistance is related to the process of epithelial-mesenchymal transition (EMT) and increased invasiveness by tongue squamous cell carcinoma (TSCC) cells. Long non-coding RNAs (lncRNAs) play pivotal roles in tumor metastasis and progression. However, the roles and mechanisms of lncRNAs in cisplatin-resistance-induced EMT and metastasis are not well understood. In this study, a chemotherapy-induced lncRNA 1 (CILA1) was discovered by using microarrays and was functionally identified as a regulator of chemo-sensitivity in TSCC cells. Upregulation of CILA1 promotes EMT, invasiveness, and chemo-resistance in TSCC cells, whereas the inhibition of CILA1 expression induces mesenchymal-epithelial transition (MET) and chemo-sensitivity, and inhibits the invasiveness of cisplatin-resistant cells both *in vitro* and *in vivo*. We also found that CILA1 exerts its functions via the activation of the Wnt/β-catenin signaling pathway. High CILA1 expression levels and low levels of phosphorylated β-catenin were closely associated with cisplatin resistance and advanced disease stage, and were predictors of poor prognosis in TSCC patients. These findings provided a new biomarker for the chemo-sensitivity of TSCC tumors and a therapeutic target for TSCC treatment.

INTRODUCTION

Tongue squamous cell carcinoma (TSCC) is the most common malignant tumor of the oral and maxillofacial region, and often progresses to local cervical lymph node metastasis.[1–3] Patients with advanced TSCC are usually treated with chemotherapy to prolong survival. However, chemotherapy resistance occurs during the course of treatment, resulting in more aggressive tumors, metastasis, and a poor prognosis.[4] Cisplatin is the most commonly used chemotherapy drug in TSCC treatment.[5,6] In a previous study, we found that cisplatin-resistant TSCC cells displayed features of epithelial-mesenchymal transition (EMT), and the upregulation of miR-200b and miR-15b reversed the mesenchymal phenotype by targeting BMI1.[7] During the EMT process, epithelial cells lose tight junctions and transition to a more invasive mesenchymal-like state, leading to enhanced motility and drug resistance.[8,9] Another study also showed that galectin-1 overexpression induces EMT in hepatocellular carcinoma cells and promotes sorafenib resistance.[10] Additionally, sparc/osteonectin, cwcv and kazal-like domain proteoglycan 1 (SPOCK1) is upregulated in temozolomide-resistant glioblastoma multiforme cells and positively regulates the EMT process.[11] Therefore, chemotherapy-induced EMT is closely associated with drug resistance, and exploring the mechanism that governs chemotherapy-induced EMT is essential for combating drug resistance.

Long non-coding RNAs (lncRNAs) are a large class of non-protein-coding transcripts that are more than 200 nt in length. lncRNAs have been shown to play important roles in cancer proliferation, apoptosis, metastasis, EMT, and drug resistance.[12] An lncRNA called the terminal differentiation-induced lncRNA (TINCR) is upregulated in gastric cancer, and SP1 may induce TINCR overexpression to regulate cell proliferation and apoptosis.[13] Dysregulation of the nuclear factor κB (NF-κB)/HOTAIR axis results in a DNA damage response and contributes to chemotherapy resistance in ovarian cancer.[14] Furthermore, LINC01133 has been shown to inhibit EMT and colorectal cancer metastasis by directly binding to the splicing factor SRSF6.15 Finally, we identified an NF-κB interacting lncRNA (NKILA), which inhibits IκB kinase (IKK)-induced IκB phosphorylation and NF-κB overactivation in inflammation-stimulated breast epithelial cells and suppresses breast cancer metastasis.[16]

Received 17 September 2017; accepted 1 April 2018;
https://doi.org/10.1016/j.ymthe.2018.04.002.

[7]These authors contributed equally to this work.

Correspondence: Jinsong Li, Department of Oral & Maxillofacial Surgery, Sun Yat-sen Memorial Hospital, Sun Yat-sen University, 107 Yanjiang West Road, Guangzhou 510120, China.
E-mail: lijinsong1967@163.com
Correspondence: Bodu Liu, Cold Spring Harbor Laboratory, Cold Spring Harbor, NY 11724, USA.
E-mail: liuleopold@gmail.com

The EMT process can be driven by many signaling pathways, including transforming growth factor β (TGF-β),[17] NF-κB,[18] Wnt/β-catenin, and others.[19] The Wnt signaling pathway can induce EMT by inhibiting the phosphorylation of glycogen synthase kinase 3β (GSK-3β) and the degradation of β-catenin in the cytoplasm. Enrichment of β-catenin in the cytoplasm can result in its translocation to the nucleus and binding to transcription factors to transactivate target genes involved in EMT and other cellular process, such as drug resistance.[20–22]

In the present study, we identified a chemotherapy-induced lncRNA 1 (CILA1), which was upregulated in cisplatin-resistant TSCC cells compared with parental cells. We found that CILA1 promotes EMT, invasiveness, and chemo-resistance in TSCC cells. To investigate the regulatory mechanism, we used mRNA microarray analysis to detect changes in gene expression caused by CILA1 overexpression in the parental cells. Notably, CILA1 increased the expression of genes in the Wnt/β-catenin signaling pathway. The silencing of CILA1 expression promoted the phosphorylation of β-catenin and inhibited β-catenin translocation into the nucleus, thereby inhibiting the activation of the Wnt/β-catenin signaling pathway. The clinical significance of CILA1 in TSCC progression was also analyzed, and the results showed that high CILA1 expression levels were related to lymph node metastasis, chemo-resistance, and poor survival in TSCC patients. Our data suggest that CILA1 promotes the metastasis and chemo-sensitivity of TSCC via the Wnt/β-catenin pathway.

RESULTS

CILA1 Is Overexpressed in Cisplatin-Resistant TSCC Cells

In addition to the cisplatin-resistant CAL-27 cell line established in our previous study,[7] we established another cisplatin-resistant TSCC cell line SCC9-res using the parental TSCC cell line SCC9. As shown in Figure S1A, the IC_{50} of CAL27-res and SCC9-res cells increased by 8- and 6.2-fold, respectively, compared with that of their parental cells. The cisplatin-induced apoptosis is significantly reduced compared with that in the parental cells. Moreover, *E-cadherin* expression was reduced, while the expression of *vimentin* was increased in CAL27-res and SCC9-res cells (Figures S1B and S1C). We then examined the invasiveness of CAL27-res and SCC9-res cells. After a 22-hr incubation, invasion and migration increased significantly in both the CAL27-res and SCC9-res cells compared with those in the respective parental cells (Figure S1D). Taken together, our observation indicates that chemoresistant CAL27-res and SCC9-res cells have undergone EMT and exhibit increased invasiveness and cellular motility.

To screen for lncRNAs that are involved in cisplatin resistance, we used lncRNA microarrays to analyze CAL27 and CAL27-res cells. As shown in the heatmap (Figure 1A), the expression levels of 66 lncRNAs were significantly upregulated in CAL27-res cells compared with that in CAL27 cells ($p < 0.05$), and the 20 lncRNAs that were upregulated more than 5-fold were chosen for further examination. We used qRT-PCR, which confirmed that the expression of seven lncRNAs was increased in CAL27-res cells and SCC9-res cells (fold change > 2; Figure 1B). To further investigate the roles of lncRNA in regulating chemo-resistance, we performed an MTS ([3-(4,5-dimethylthiazol-2-yl)-5-(3-carboxymethoxyphenyl)-2-(4-sulfophenyl)-2H-tetrazolium) assay in CAL27-res cells and SCC9-res cells using small interfering RNAs (siRNAs) that specifically targeted each of the seven lncRNAs. We found that only the silencing of CILA1 expression significantly increased the cisplatin sensitivity of chemoresistant cells (Figure 1C). Based on the above results, we hypothesized that high expression levels of the lncRNA CILA1 are associated with chemoresistance and EMT of TSCC cells.

CILA1 Promotes EMT and Chemo-resistance in TSCC Cells

We identified and cloned the full length of CILA1 transcript using 5′ and 3′ rapid amplification of cDNA end (RACE; Figure S2). CILA1 was found to be a 709-nt transcript and did not appear to have a protein-coding open reading frame (ORF) (no ORF longer than 300 nt). To further examine the functions of CILA1, we silenced CILA1 expression in CAL27-res and SCC9-res cells (Figure 2A), and we found that reduction of CILA1 increased *E-cadherin* expression and inhibited *vimentin* expression in both CAL27-res and SCC9-res cells as shown by western blot, qRT-PCR, and immunofluorescence staining assays (Figures 2B–2D). In addition, invasion and migration of CAL27-res and SCC9-res cells were remarkably reduced by silencing CILA1 expression (Figure 2E; Figures S3A and S3B). Reduction of CILA1 expression reversed the mesenchymal features of cisplatin-resistant TSCC cells.

To evaluate whether reduction in CILA1 was associated with chemo-resistance, we examined apoptosis of TSCC cells using the TUNEL assay and Annexin V/propidium iodide (PI) staining. Although treatment with cisplatin did not obviously increase the percentage of apoptotic CAL27-res and SCC9-res cells, inhibition of CILA1 expression resulted in a significant increase in apoptotic cells in the presence of cisplatin (Figures 2F and 2G; Figures S3C and S3D). Moreover, knockdown of CILA1 expression also reduced cell viability in the treatment with cisplatin in both CAL27-res and SCC9-res cells (Figure 2H), suggesting that downregulation of CILA1 can increase the sensitivity of resistant TSCC cells to chemotherapy.

Next, we ectopically expressed CILA1 in CAL27 and SCC9 cells (Figure 3A). Overexpression of CILA1 suppressed *E-cadherin* expression and enhanced *vimentin* expression in CAL27 and SCC9 cells (Figures 3B–3D). The invasion and migration of parental cells were also increased by ectopic expression of CILA1 (Figure 3E; Figures S4A and S4B). Furthermore, sensitivity to cisplatin in CAL27 and SCC9 cells was strongly inhibited by CILA1. The numbers of apoptotic cells were decreased, and cell viabilities were increased by CILA1 after treatment with cisplatin (Figures 3F and 3H; Figures S4C and S4D). Collectively, these data suggest that the lncRNA CILA1 promotes EMT, invasiveness, and chemo-resistance in TSCC cells.

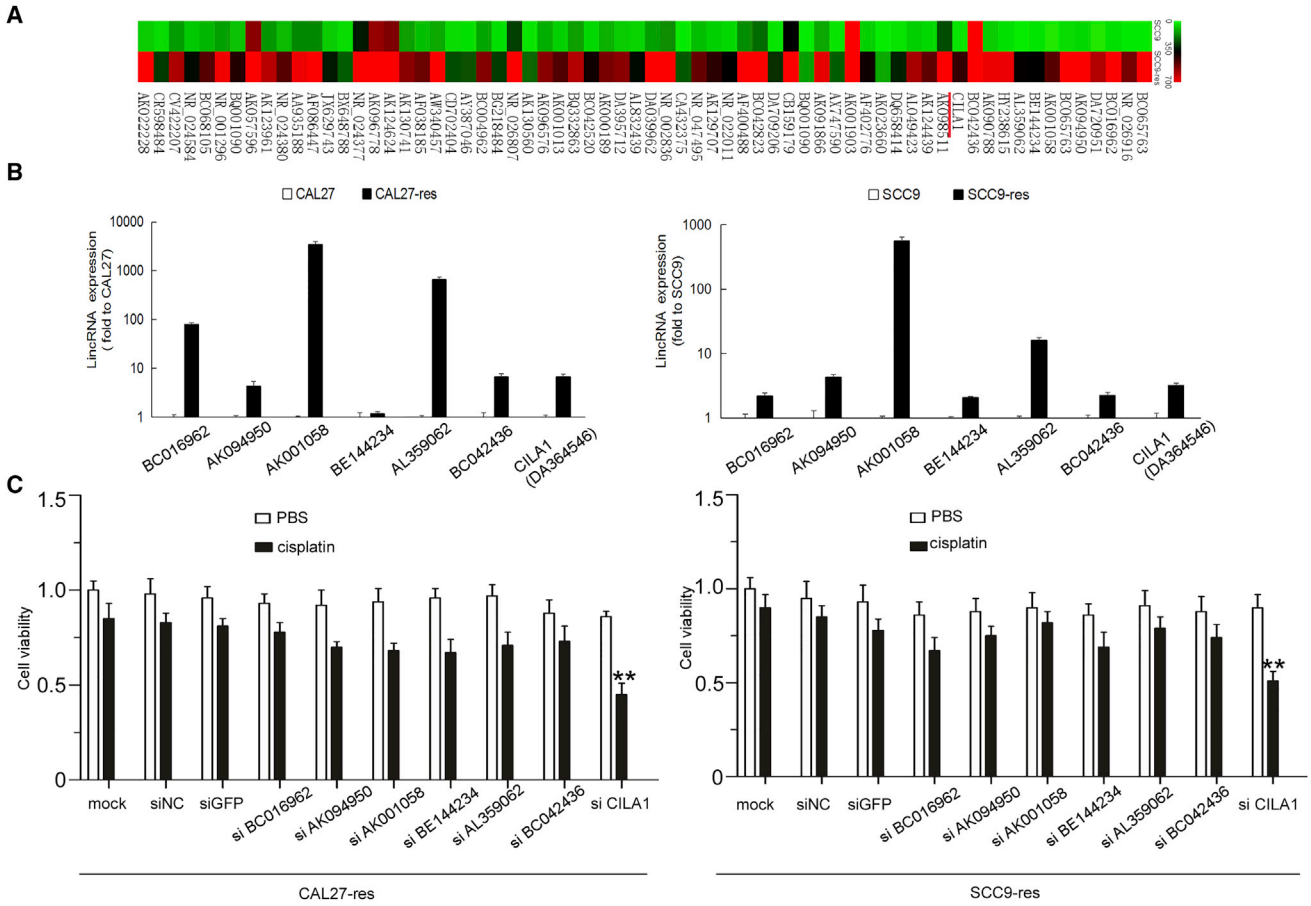

Figure 1. lncRNA CILA1 Was Remarkably Differentially Expressed in Cisplatin-Resistant TSCC Cells

(A) SCC9 cells were treated with cisplatin to establish chemoresistant cell lines, and the lncRNA differential expression profiles were analyzed by microarray. The mean fluorescence intensity was calculated and displayed as the average level. The results are presented as the lncRNA expression ratio of SCC9 chemoresistant versus the SCC9 parental cells. (B) Real-time qPCR was performed to examine the expression of the most remarkably upregulated lncRNAs in cisplatin-resistant cells compared with those in parental cells. (C) An MTS assay was performed to determine the cell viability of TSCC chemoresistant cells with knocked down lncRNA expression (**p versus mock < 0.01).

CILA1 Activates the Wnt/β-Catenin Signaling Pathway in TSCC Cells

To study the mechanism by which CILA1 promotes chemotherapy-induced EMT, we used mRNA microarray to study SCC9 cells with or without CILA1 overexpression. Overexpression of CILA1 significantly increased the expression of a panel of genes in the Wnt signaling pathway, which are associated with tumorigenesis,[23] EMT,[24] and enhanced cancer metastasis.[25,26] The top 15 upregulated genes were chosen for further verification (Figure 4A). qRT-PCR verified that *Wnt5A* expression was mostly increased by CILA1 (Figure 4B). Thus, we examined whether CILA1 activated the Wnt/β-catenin pathway in TSCC cells. Strikingly, subcellular fractionation and immunofluorescence assays showed that the chemo-resistant TSCC cells, which expressed high levels of CILA1, express high-level total β-catenin, accompanied by translocation of cytoplasmic β-catenin to the nucleus (Figures 4C and 4D). Because the inhibition of GSK-3-mediated β-catenin phosphorylation and degradation is crucial for Wnt/β-catenin signaling activation,[27–30] we also examined the phosphorylation of β-catenin and GSK-3β in TSCC cells. We found that phosphorylation of GSK-3β (Ser9) was much higher, yet phosphorylation of β-catenin was much lower in CAL27-res and SCC9-res cells, compared with CAL27 and SCC9 cells, respectively (Figure 4C).

In addition, forced upregulation of CILA1 in TSCC parental CAL27 and SCC9 cells and upregulation of CILA1 resulted in an increase in total β-catenin expression and its translocation from the cytoplasm to the nucleus. In addition, overexpression of CILA1 also increased the phosphorylation of GSK-3β, without affecting the total level of GSK-3β (Figure 4E). However, in TSCC chemo-resistant cells, reduction of CILA1 inhibited GSK-3β phosphorylation, enhanced β-catenin phosphorylation, and decreased nuclear accumulation of β-catenin (Figure 4E). We also examined the expression of downstream signaling molecules of the Wnt/β-catenin pathway, including c-Myc and survivin. Ectopic expression of CILA1 increased the expression, while

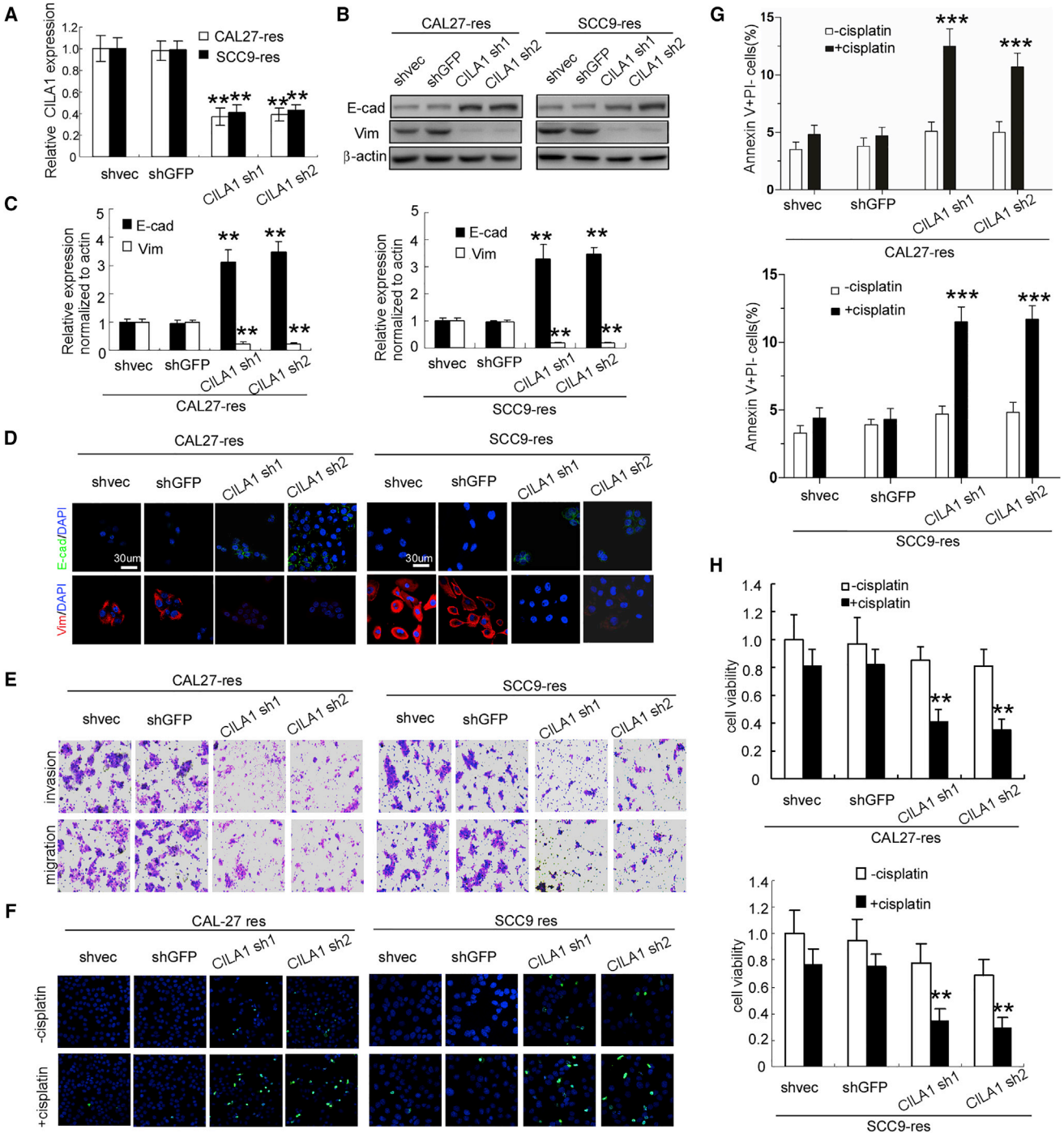

Figure 2. The Silencing of CILA1 Expression Inhibits Resistant TSCC Cell Proliferation, Invasion, Anti-apoptosis, and EMT

(A) Real-time qPCR was performed to determine the silencing efficiency of CILA1 in TSCC cells. Western blot (B), real-time qPCR (C), and immunofluorescence (D) analyses were performed to examine the changes in EMT marker expression with CILA1 silencing. (E) Boyden chamber assays were explored to examine the change in TSCC cell motility after knockdown of CILA1 expression. TUNEL (F) and flow cytometry (G) assays were performed to determine the anti-apoptotic effect of CILA1. (H) An MTS assay was performed to examine the viability of TSCC chemoresistant cells with knocked down CILA1 expression (**$p < 0.01$; ***$p < 0.001$).

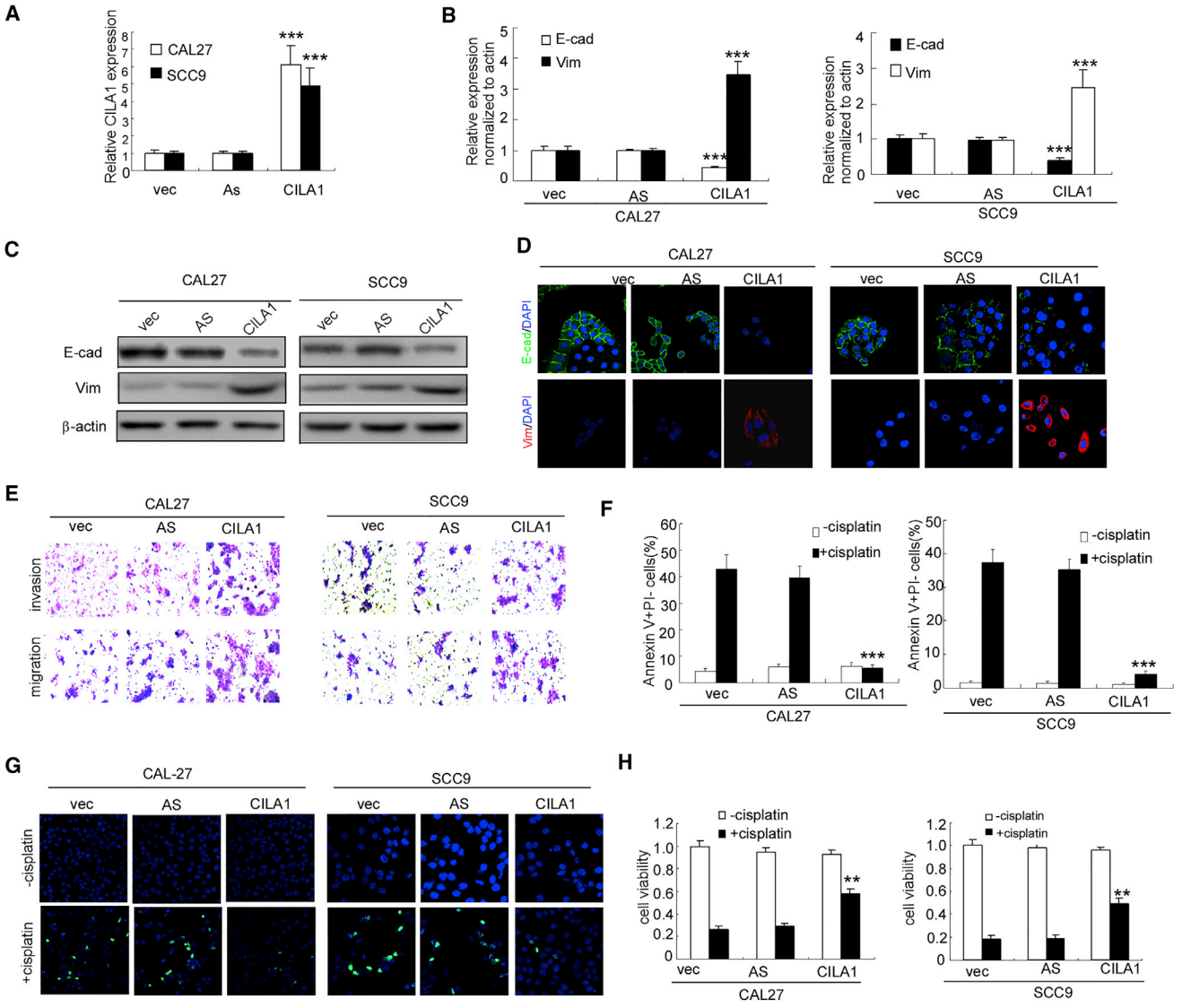

Figure 3. Ectopic Expression of CILA1 Enhances Cisplatin-Sensitive TSCC Cell Proliferation, Invasion, Anti-apoptosis, and EMT

(A) The overexpression efficiency was determined by real-time qPCR in cisplatin-sensitive TSCC cells. Quantitative real-time PCR (B), western blot (C), and immunofluorescence assays (D) were performed to examine the changes in EMT marker expression upon upregulation of CILA1. (E) Boyden chamber assays were explored to examine the changes in TSCC cell motility after CILA1 overexpression. Flow cytometry (F) and TUNEL assays (G) were performed to determine the anti-apoptotic effect of the CILA1 upregulation. (H) An MTS assay was performed to examine chemoresistant TSCC cell viability with overexpressed CILA1 (**$p < 0.01$; ***$p < 0.001$).

silencing CILA1 significantly reduced the expression of these targets (Figure 4E). These observations suggest that CILA1 enhances expression of *WNT5A*, promotes nuclear accumulation of β-catenin, and then activates the Wnt/β-catenin signaling pathway in TSCC cells.

CILA1 Regulates EMT and Chemo-Resistance in TSCC Cells via the Wnt/β-Catenin Signaling Pathway

To further explore whether the lncRNA CILA1 exerts its functions by regulating the Wnt/β-catenin signaling pathway, we used the Wnt/β-catenin agonist (GSK-3 inhibitor) CHIR99021 to perform a rescue experiment in the CAL27-res and SCC9-res cell lines. We have known that reduction of CILA1 inhibits the activation of the Wnt/β-catenin signaling pathway in chemo-resistant TSCC cells (Figures 4E and 5A). However, in the presence of CHIR99021, GSK-3β could no longer phosphorylate β-catenin, and the total expression and nuclear translocation of β-catenin were increased. The expressions of c-Myc and survivin were activated (Figure 5A). CHIR99021 rescued the inhibition of the Wnt/β-catenin pathway caused by silencing CILA1.

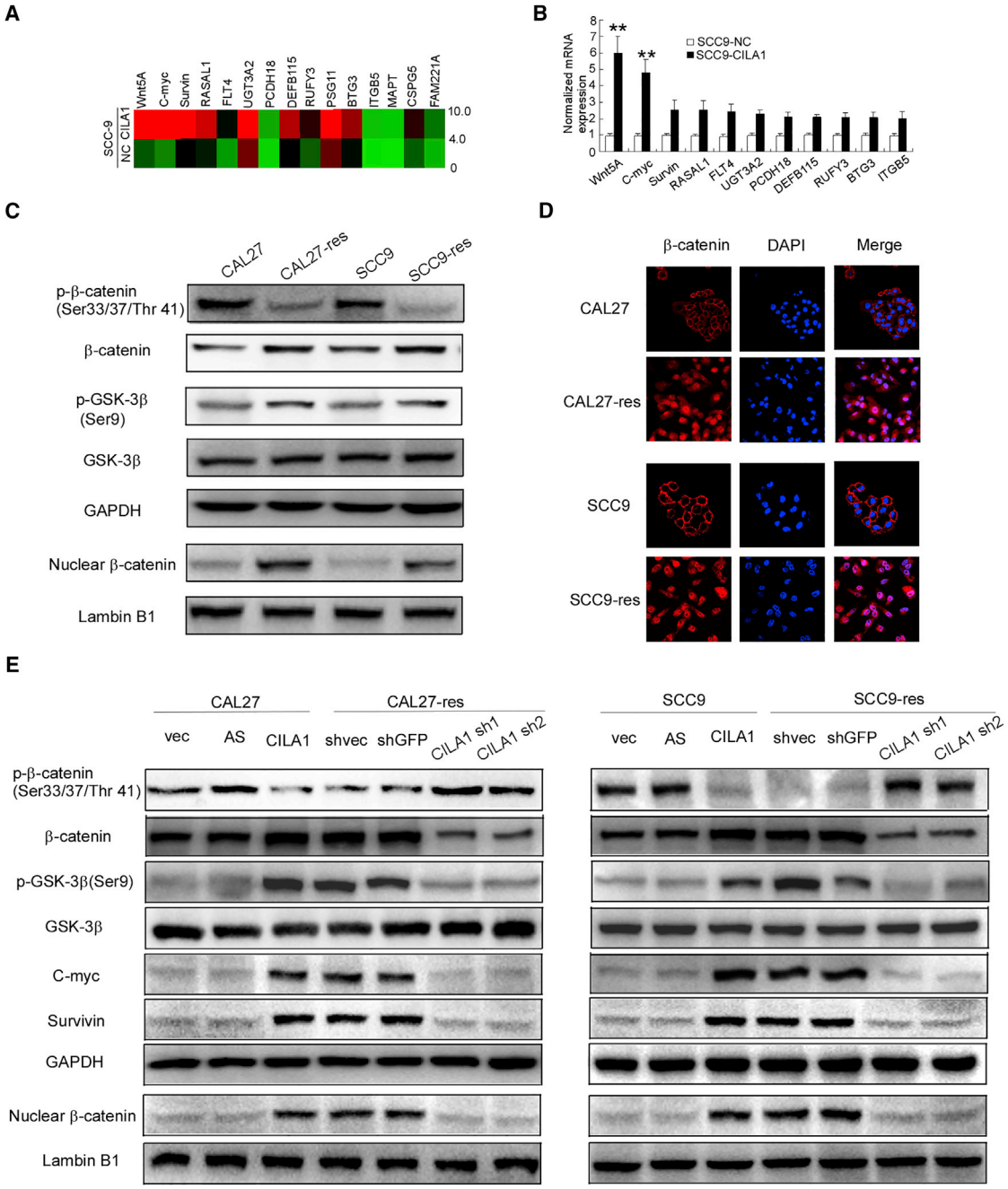

Figure 4. The Wnt/β-Catenin Signaling Pathway Was Activated in Chemoresistant TSCC Cells

(A) mRNA microarray analysis was performed to reveal differential mRNA expression in SCC-9 cells overexpressing CILA1 compared with that in SCC-9 control cells. (B) Real-time qPCR was used to confirm the differences in mRNA expression observed in the mRNA microarray. The data are representative of three independent experiments. (C) Total and p-β-catenin, GSK-3β, and nuclear β-catenin expression were assayed by western blotting. GAPDH and lamin B1 were used as controls. (D) An immunofluorescence assay was performed to determine the subcellular β-catenin expression and localization. (E) Upregulation of CILA1 increased total β-catenin, phosphorylated β-catenin, GSK-3β, AKT, Survivin, and c-Myc expression, while the silencing of CILA1 expression had the opposite effects, as assayed by western blotting. GAPDH and lamin B1 were used as controls. $^{**}p < 0.01$.

We examined the influences of CHIR99021 on cell motility and chemo-resistance in TSCC cells. We found that addition of CHIR99021 promotes invasion and migration of CAL27-res and SCC9-res cells, when CILA1 expression is silenced (Figure 5B; Figures S5A and S5B). In addition, CHIR99021 increased *vimentin* expression and inhibited *E-cadherin* expression in these cells

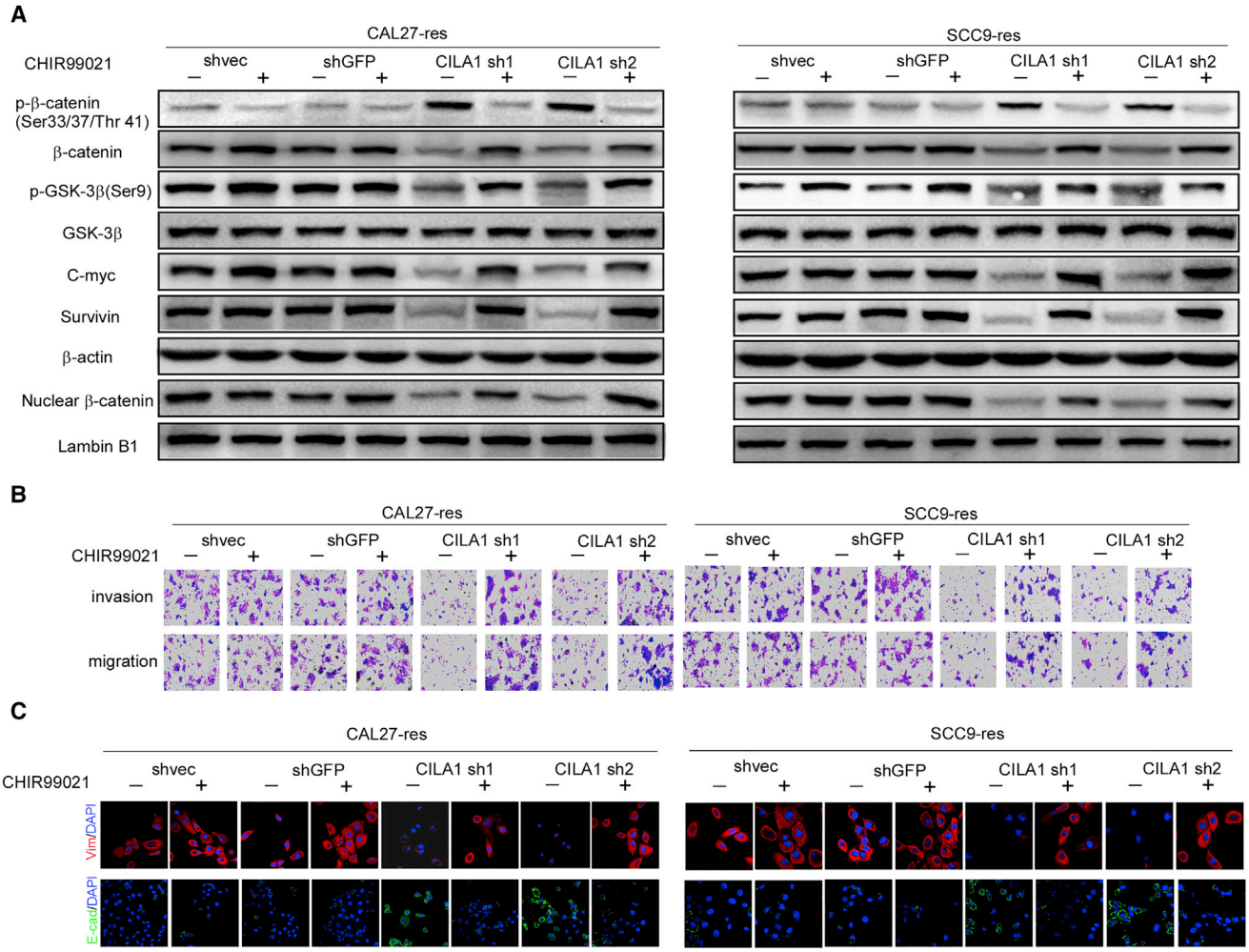

Figure 5. CILA1 Promotes TSCC EMT and Metastasis via the Wnt/β-Catenin Signaling Pathway

(A) After stable silencing of CILA1 expression, chemoresistant TSCC cells were treated with CHIR99021 (6 μmol/L) for 24 hr; then the indicated protein expression levels were examined using western blotting. Knockdown of CILA1 expression inhibited expression of these proteins, while CHIR99021 partially rescued the expression level. β-Catenin and lamin B1 were used as controls. (B) Invasion and migration assays demonstrated the invasiveness of the TSCC cells with stable silencing of CILA1 expression and treated with CHIR99021 (6 μmol/L) for 24 hr. Inhibition of CILA1 expression impaired TSCC cell motility, and CHIR promoted it. (C) Expression of EMT markers was determined in TSCC cells with stable silencing of CILA1 expression using immunofluorescence analysis. The silencing of CILA1 expression enhanced E-cadherin expression and attenuated vimentin expression. CHIR99021 reversed the EMT process.

(Figure 5C; Figures S5C and S5D). TUNEL assay and Annexin V/PI staining showed that CHIR99021 decreased apoptotic cell numbers in CAL27-res and SCC9-res cells with silenced CILA1 expression that were treated with cisplatin (Figures 6A and 6B; Figures S5E and S5F). Moreover, in the presence of CHIR99021, knockdown of CILA1 expression could not reduce cell viability in CAL27-res and SCC9-res cells any longer in the treatment with cisplatin (Figure 6C). Taken together, these results show that Wnt/β-catenin agonist CHIR99021 rescued the effects of silencing CILA1 on the invasiveness and chemo-resistance of the cells, suggesting that the lncRNA CILA1 regulates EMT and chemo-resistance in TSCC cells via the Wnt/β-catenin signaling pathway.

Expression Levels of CILA1 Influence Metastasis of TSCC Xenografts

Because silencing CILA1 expression inhibits the cell motility of chemo-resistant TSCC cells *in vitro*, we further assessed its effect on tumor growth and metastasis *in vivo*. TSCC cells were injected subcutaneously into the armpit of nude mice. Reduction of CILA1 remarkably suppressed tumor growth of SCC9-res xenografts with the treatment of cisplatin (Figures 7A and 7B). To explore the effect of CILA1 on tumor apoptosis, we performed a TUNEL assay. We found that inhibiting CILA1 expression promoted apoptosis in TSCC cells that were treated with cisplatin (Figure 7C). Furthermore, reduction of CILA1 inhibited liver and lung metastases of SCC9-res xenografts (Figure 7D). These results suggest that reduction of

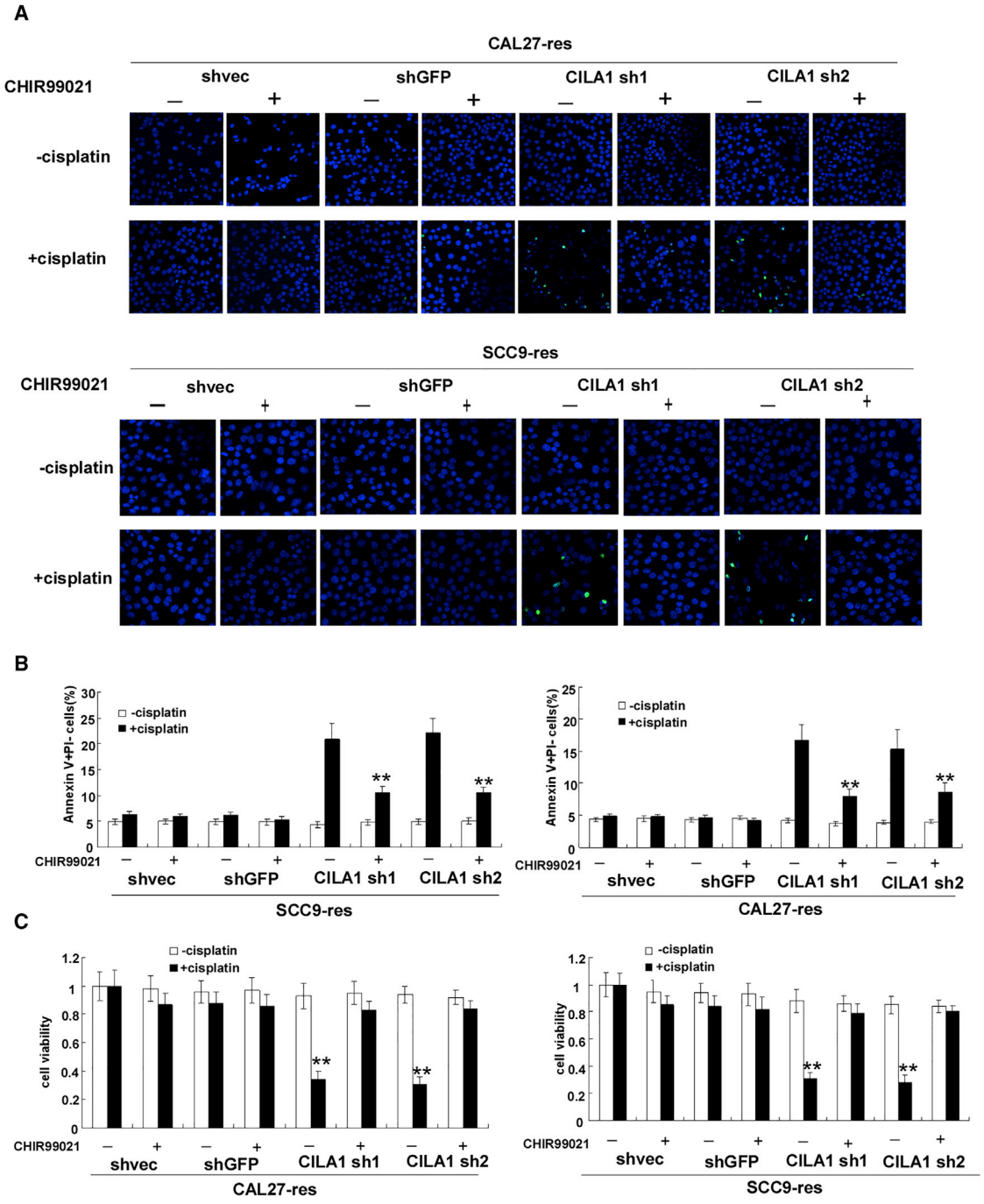

Figure 6. The Wnt/β-Catenin Signaling Pathway Mediates CILA1-Induced Chemoresistant TSCC Cell Anti-apoptosis and Proliferation

(A) TUNEL analysis showed that the silencing of CILA1 expression impaired the TSCC anti-apoptotic abilities induced by cisplatin, while CHIR 99021 reversed this effect. (B) The percentage of apoptotic cells was determined by flow cytometry, and CILA1 inhibition enhanced TSCC cell apoptosis induced by cisplatin, while CHIR99021 partially attenuated this effect. (C) Knockdown of CILA1 impaired the TSCC cell growth rate upon cisplatin treatment, as determined by an MTS assay, while CHIR99021 rescued TSCC cell proliferation (**$p < 0.01$; ***$p < 0.001$).

CILA1 can increase chemo-sensitivity and inhibit metastasis in TSCC tumors. Upregulation of CILA1 strongly promoted the tumor growth of SCC9 xenografts (Figure 7E) and inhibited the apoptosis of TSCC cells that were treated with cisplatin (Figure 7G). Furthermore, upregulation of CILA1 promoted liver and lung metastases of SCC9 xenografts (Figure 7F).

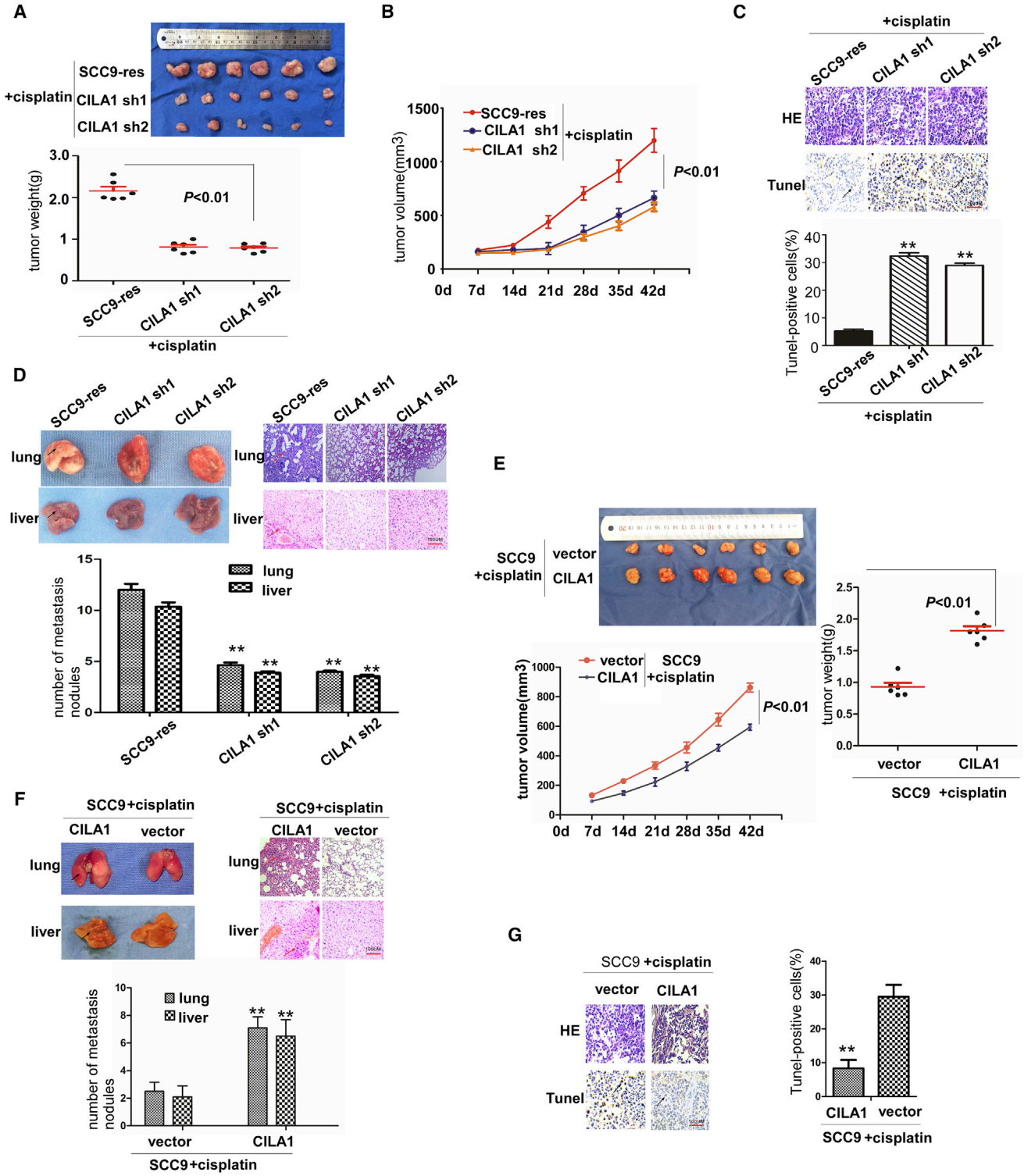

Figure 7. CILA1 Knockdown Inhibits TSCC Cell Growth and Metastasis *In Vivo* upon Cisplatin Treatment

(A) A total of 1 × 10^6 stable CILA1-knockdown SCC9 cells were subcutaneously injected into the axilla of nude mice (n = 6 for both groups). Tumor weights were calculated at the sixth week. (B) Tumor volume was measured every week. (C) The number of apoptotic cells was determined by TUNEL assay on mouse tumor slides. (D) Lung and liver

(legend continued on next page)

Upregulation of CILA1 in TSCC Correlates with Chemotherapeutic Resistance and Poor Patient Survival

We further evaluated the clinical significance of CILA1 expression in TSCCs. According to previous studies, TSCCs can be classified as cisplatin-resistant tumors or cisplatin-sensitive tumors. The studied TSCC patients all received chemotherapies. The treatment periods are equal before surgery. Samples collected from TSCC patients included normal adjacent tissues, TSCC sensitive and TSCC resistant. *In situ* hybridization and immunohistochemical staining showed that expressions levels of CILA1 and vimentin were low, and expressions levels of phosphorylated β-catenin (p-β-catenin) and E-cadherin were high in normal tongue samples (Figure 8A).The expression of CILA1 was increased in cisplatin-sensitive TSCC tumors and was highest in cisplatin-resistant tumors, and the level of p-β-catenin was lowest in cisplatin-resistant tumors. The expression difference between chemo-sensitive and chemo-resistant TSCCs, as determined by the percentage of positive cells, was significant (Figure 8B; $p < 0.01$). In addition, Spearman correlation analysis showed that CILA1 expression in TSCCs was negatively correlated with p-β-catenin expression (Figure 8C; $r = -0.845$; $p < 0.001$).

Next, we analyzed the association of CILA1 and p-β-catenin expression with clinicopathological status in TSCC patients (Table 1). There was no significant correlation between CILA1 or p-β-catenin level and the patient's sex, age, or clinical stage. However, levels of CILA1 expression and p-β-catenin were significantly correlated with node metastasis and cisplatin sensitivity in TSCC patients, respectively. Tumors with lymph node metastasis or cisplatin resistance expressed a high level of CILA1 and a low level of p-β-catenin.

Furthermore, we evaluated the correlation between CILA1 expression and patient survival. Patients with low expression of CILA1 in tumors survived significantly longer than those with high CILA1 expression in tumors ($p = 0.000$; Figure 8D). Conversely, high levels of p-β-catenin level were associated with better survival ($p = 0.005$; Figure 8E). These data suggest that CILA1expression is positively correlated with tumor stage and may play a role in the progression of TSCCs.

DISCUSSION

This study sought to determine the molecular mechanism by which the lncRNA CILA1 promotes tumor progression in human TSCC. Our results suggest that CILA1 can activate the Wnt/β-catenin signaling pathway to promote EMT and chemo-resistance, leading to an aggressive phenotype and tumor metastasis. Metastasis is the main factor leading to mortality in TSCC patients, and both EMT and chemo-resistance contribute to cancer metastasis.[30,31]

For the past decade, lncRNAs have been shown to participate in a variety of biological processes in malignant tumors including metastasis, EMT, drug resistance, and so on. In HER2-positive breast cancers, trastuzumab resistance often occurs, and Shi et al.[32] found that lnc-ATB was upregulated in drug-resistance breast cancer cells and trastuzumab resistance tissues. Further research found that lnc-ATB could competitively bind miR-200c and then induce EMT.[32] In studies on gastric cancer drug resistance, LEIGC was found to have reduced expression in human gastric cancers compared with adjacent non-cancerous tissues. Upregulating LEIGC expression promotes the sensitivity of gastric cancer cells to fluorouracil (5-FU) and inhibits the process of EMT.[33]

In the present study, identified lncRNA named CILA1 was found to be an important biomarker in tongue cancer drug resistance and was found to be correlated with the process of EMT. Further mechanistic studies found that Wnt/β-catenin signaling is activated by CILA1. The Wnt/β-catenin signaling is related to chemo-resistance, metastasis, and EMT in multiple tumors. Previous studies have shown that the Wnt signaling pathway can be divided into two categories, including the canonical Wnt pathway and non-canonical Wnt pathways. The activation of canonical Wnt signaling involves the degradation of β-catenin and the transcription of target genes. The non-canonical signaling Wnt pathway can induce EMT conversion by inhibiting the phosphorylation of *GSK3β* independent of *β-catenin*. A large increase in intracellular abundance of β-catenin will be transferred into the nucleus, as a transcription factor subunit to induce the expression of a large number of genes, many of which are transcription factors that activate EMT.[34]

Increased Wnt/β-catenin pathway activity plays an important role in chemoresistance. Peng et al. [35] found that the lncRNA CRNDE can regulate colorectal cancer chemo-resistance by affecting the expression of miR-181a-5p and finally influencing Wnt/β-catenin signaling. In research on ovarian cancer chemo-resistance, Anastas et al.[36] found that upregulation of the expression of WNT5A in SKOV3/Wnt5a cells reduced the chemo-sensitivity of the cells. WNT5A expression is increased in BRAFi-resistant melanomas, and a reduction of endogenous WNT5A leads to increased apoptosis when treated with BRAFi.[37] In the present study, CILA1 increased the expression of *WNT5A* and regulated expression and phosphorylation of *β-catenin*, then activated the canonical wnt pathway.

Identifying and revealing the underlying mechanisms that activate EMT may shed light on novel therapeutic strategies that could be used to suppress tumor progression. Several studies have demonstrated that EMT-induced dysregulation of signaling cascades, such as the Wnt/β-catenin signaling cascade, might be associated with tumorigenesis and cancer progression.[38–40] The translocation

were collected and analyzed in the negative control group and the CILA1-knockdown group. The number of metastatic nodules in the liver and lung was calculated. (E) A total of 1×10^6 stable CILA1-overexpression SCC9 cells were subcutaneously injected into the axilla of nude mice (n = 6 for both groups). Tumor weights were calculated at day 42. Tumor volume was measured every week. (F) Lung and liver were collected and analyzed in the negative control group and the CILA1-overexpression group. The number of metastatic nodules in the liver and lung was calculated. (G) The number of apoptotic cells was determined by TUNEL assay on mouse tumor slides (**$p < 0.01$).

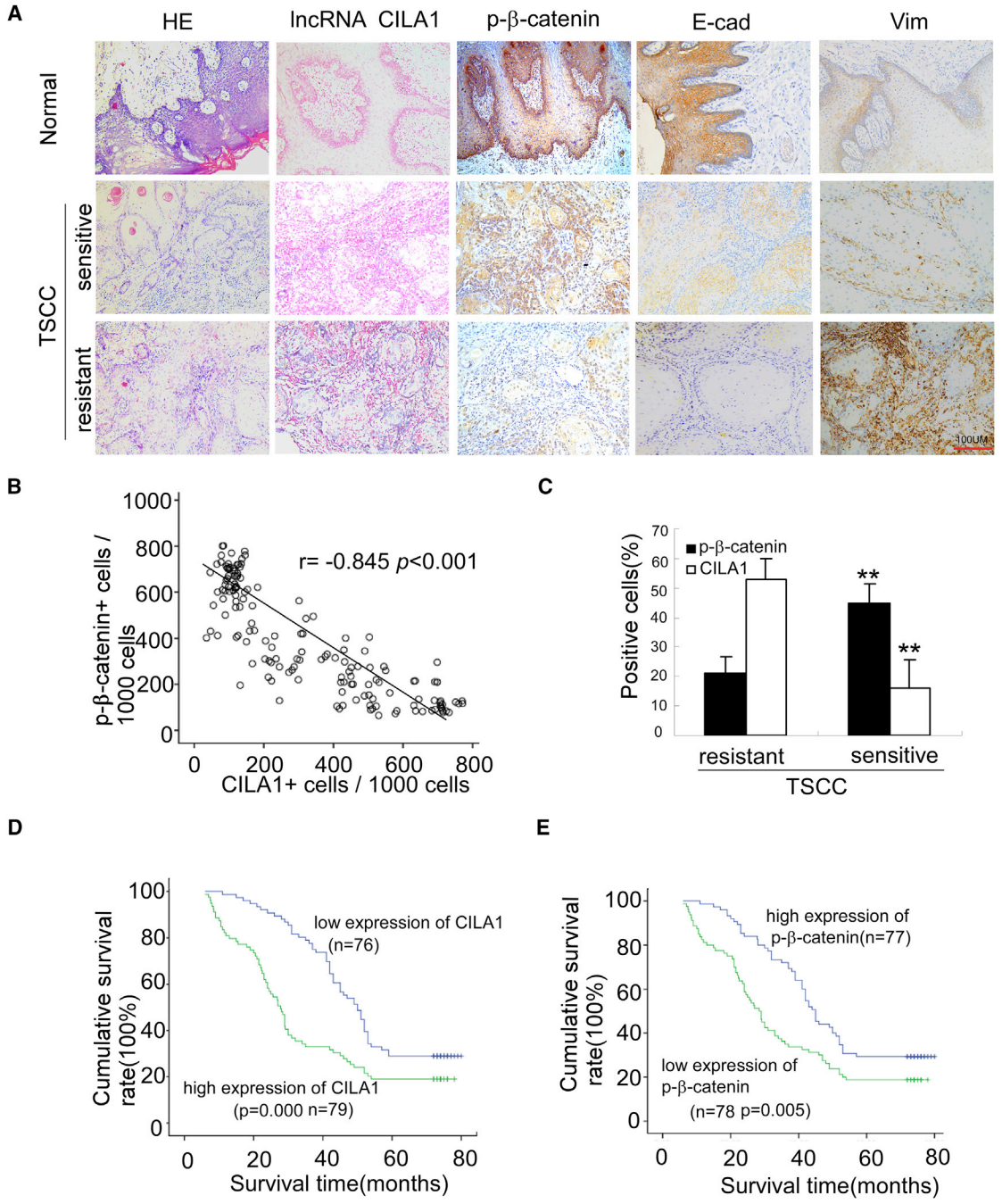

Figure 8. CILA1 Upregulation Is Associated with Metastasis and Poor Survival in TSCC Patients

(A) *In situ* hybridization for CILA1 and immunohistochemical staining for p-β-catenin, E-cadherin, and vimentin were examined in non-tumor and tumor tissues with and without metastasis. Scale bars, 100 μm. (B) Associations between CILA1 and p-β-catenin expression in TSCCs were analyzed by Spearman analysis. (C) Quantification of CILA1 and p-β-catenin expression in tumor tissues with and without metastasis in TSCC patients (**p < 0.01). Kaplan-Meier survival curves are plotted and analyzed by log-rank test for TSCC patients associated with the expression of CILA1 (D) and p-β-catenin (E).

of β-catenin from the cytoplasm to the nucleus led to down-regulation of E-cadherin and the induction of EMT. However, the attenuation of Wnt/β-catenin signaling can inhibit EMT transcription factor expression. Therefore, determining how oncogenes might regulate this pathway may provide new insights into the molecular mechanisms underlying EMT and cancer metastasis, and may further facilitate the development of novel anti-metastatic strategies.

Table 1. Correlation among Clinicopathological Status between the Expression of lncRNA CILA1 and p-β-Catenin in TSCC Patients

	lncRNA CILA1 (%)			p-β-Catenin (%)		
Characteristics	No. of High Expression	No. of Low Expression	p Value	No. of High Expression	No. of Low Expression	p Value
Sex						
Male	48 (50.1)	46 (49.9)	0.976	43 (45.7)	51 (54.3)	0.224
Female	31 (50.8)	30 (49.2)	0.976	34 (55.7)	27 (44.3)	0.224
Age						
<50 years	22 (52.4)	20 (47.6)	0.830	19 (45.2)	23 (54.8)	0.500
≥50 years	57 (50.4)	56 (49.6)	0.830	58 (51.3)	55 (48.7)	0.500
Node Metastasis						
N0	30 (39.5)	46 (60.5)	0.005	31 (40.8)	45 (59.2)	0.03
N+	49 (62.0)	30 (38.0)	0.005	46 (58.2)	33 (41.8)	0.03
Clinical Stage						
III	28 (38.9)	44 (61.1)	0.005	27 (37.5)	45 (62.5)	0.002
IV	51 (61.4)	32 (38.6)	0.005	50 (60.2)	33 (39.8)	0.002
Status						
Survival	13 (37.1)	22 (62.9)	0.000	15 (42.9)	20 (57.1)	0.011
Death	66 (55.0)	54 (45.0)	0.000	62 (51.7)	58 (48.3)	0.011
Cisplatin						
Sensitive	24 (35.3)	44 (64.7)	0.005	24 (35.3)	44 (64.7)	0.004
Non-sensitive	55 (63.2)	32 (36.8)	0.005	53 (60.9)	34 (39.1)	0.004

MATERIALS AND METHODS

Clinical Specimens, Cell Culture, and Cell Transfection

A total of 155 patients were recruited for this study from three independent centers, including Sun Yat-sen Memorial Hospital (n = 104), the West China Hospital (n = 18), and the Affiliated Hospital of North Sichuan Medical College (n = 33), between May 2006 and August 2012. Patients' responses to treatment were classified as cisplatin sensitive or resistant according to previous studies. The tumor samples were examined by two independent pathologists, and the grade was defined according to World Health Organization (WHO) criteria (2004). The clinicopathological characteristics are summarized in Table 1. This study was approved by the ethics boards of the three hospitals, and all patients provided informed consent.

Two TSCC cell lines, CAL27 and SCC9, were used in this study. Both cell lines were obtained from the ATCC. To construct stable cisplatin-resistant cell lines, we treated CAL27 and SCC9 cells with cisplatin (Sigma, St. Louis, MO, USA) with concentrations that gradually increased from 10^{-7} to 10^{-5} M. CAL27 and CAL27-res cells were maintained in DMEM (GIBCO, Rockville, MD, USA) supplemented with 10% fetal bovine serum (Invitrogen, Carlsbad, CA, USA). SCC9 and SCC9-res cells were cultured in DMEM-F12 (GIBCO) supplemented with 10% fetal bovine serum and 400 ng/mL hydrocortisone (Sigma).

For cell transfection, all siRNAs and lentiviruses against CILA1 and the negative controls were synthesized and purchased from Ribobio (Guang Zhou, China) (Table S1). TSCC cells were transfected with siRNAs using Lipofectamine 3000 (Invitrogen) according to the manufacturer's protocols, and lentiviral production and transduction were performed according to the manufacturer's instruction. The gene silencing efficiency was analyzed by qRT-PCR after infection for 48 hr.

Cell Viability, Proliferation Assay, and Apoptosis Assay

Cells were collected and seeded into 96-well plates at a concentration of 10,000 cells/mL. Cell viability was evaluated by an MTS assay as recommended by the manufacturer (Promega, Tokyo, Japan). In brief, 20 μL of MTS solution was added to each well followed by a 1-hr incubation at 37°C. The purple product of the reaction was quantitatively measured in a Microplate Reader (Synergy H1 Hybrid Multi-Mode BioTek, Winooski, VT, USA) at a 490-nm wavelength.

For the TUNEL assay, apoptotic DNA fragmentation was examined using a kit from Roche (Cat. No. 11684795910) according to the manufacturer's protocol. In brief, cells were plated in 24-well flat-bottom plates after transfection and fixed in 4% paraformaldehyde at room temperature for 15 min. Then, cells were permeabilized in 0.1% Triton X-100 and labeled with fluorescein-12-deoxyuridine triphosphate (dUTP) using terminal deoxynucleotidyl transferase, and sections were examined with an Imager Z1 microscope (Zeiss, Jena, Germany). An investigator blind to the treatment quantified 20 random fields of samples. For flow cytometry, TSCC cells were stained with FITC-Annexin V (AV) and PI on ice and then analyzed with a flow cytometer (fluorescence-activated cell sorting [FACS]; BD Biosciences, San Jose, CA, USA).

lncRNA Microarray and qRT-PCR

lncRNA microarray analyses were compared between SCC9 and SCC9-res cells. The differentially expressed lncRNAs in SCC9 versus SCC9-res cells were calculated, identified, and visualized in a heatmap using DMVS 2.0 software (KangchengBio Corporation, Shanghai, China).

qRT-PCR was performed with the LightCycler Real-Time PCR System (Roche Diagnostics, Switzerland). Reactions were run in triplicate in three independent experiments, and glyceraldehyde-3-phosphate dehydrogenase (*GAPDH*) was used as the control. Primers for genes involved in qRT-PCR are listed in Table S1.

Western Blot Analysis and Immunofluorescence Staining

Equal quantities of protein were separated via 10% SDS-PAGE gel. The proteins were then transferred to polyvinylidene difluoride membranes (Amersham Pharmacia Biotech) and probed with primary antibodies, followed by incubation with a peroxidase-conjugated secondary antibody (Proteintech) and visualization with an enhanced chemiluminescence kit (GE, Fairfield, CT, USA) according to the manufacturer's instructions. GAPDH was used as a loading control. Primary antibodies used in the study are listed in Table S2.

Cells were cultured and treated on coverslips. After fixation and permeabilization, the cells were incubated with primary antibodies and then incubated with Alexa 594 and Alexa 488 conjugated with secondary antibodies (Invitrogen). The coverslips were counterstained with DAPI and imaged under an SLM780 confocal microscope (Zeiss, Germany).

Boyden Chamber Assay

A total of 1×10^5 cells were added to the upper chamber of a polycarbonate transwell filter (Corning) and incubated for 22 hr. For the invasion assay, the upper chambers were precoated with Matrigel (BD, Minneapolis, MN, USA). The non-invading cells on the lower membrane surface were scratched, fixed with 4% paraformaldehyde, stained with crystal violet, photographed, imaged, and counted.

RACEs

We used a SMARTerRACE cDNA Amplification Kit (Clontech, Palo Alto, CA, USA) to find the transcriptional initiation and termination sites of CILA1 according to the manufacturer's instructions. PCR products were obtained and then cloned into pEASY-T3 (TransGen Biotech, Beijing, China) for further sequencing.

Tumor Xenografts

A total of 1×10^6 cells were subcutaneously injected into the axilla of BALB/c-nu mice, and the tumor size was measured and calculated as follows: Volume (mm^3) = length $\times$ width^2 $\times$ 0.5. After the mice were sacrificed, tumor xenografts and the lung and liver were harvested, weighed, and frozen in liquid nitrogen. To evaluate *in vivo* metastasis, we stained the lung and liver tissues with H&E and used them for immunohistochemistry.

In Situ Hybridization and Immunohistochemistry

An *in situ* hybridization assay was performed in primary TSCC samples according to the manufacturer's protocol (Exiqon, Vedbaek, Denmark). In brief, after demasking, CILA1 was hybridized to 5′ digoxigenin (DIG)-labeled locked nucleic acid (LNA) probes on the slides. Then, the DIG was incubated with a specific anti-DIG antibody conjugated to alkaline phosphatase, and the nuclei were counterstained with nuclear fast red. A total of 5 $\times$ 200 tumor cells were counted randomly in each section: high-expression, positive cells $\geq$30%, and low-expression, positive cells <30%.[7]

Immunohistochemistry was performed on the paraffin-embedded primary TSCC tissue sections. The tissue sections were incubated with a primary antibody at 4°C overnight. For the negative controls, isotype-matched antibodies were applied. The sections were then treated with a secondary antibody, followed by further incubation with a streptavidin-horseradish peroxidase complex. Diaminobenzidine (Dako, Carpinteria, CA, USA) was used as a chromogen, and the nuclei were counterstained with hematoxylin. The tissue sections were observed under a Zeiss AX10-Imager A1 microscope (Carl Zeiss, Thornwood, NY, USA), and all images were captured using AxioVision 4.7 microscopy software (Carl Zeiss, Thornwood, NY, USA). Tumor cells (5 $\times$ 200) were counted in each section: high-expression, positive cells $\geq$35%, and low expression, positive cells <35%.[7]

Statistical Analysis

All statistical analyses were performed using SPSS 19.0 software (SPSS, Chicago, IL, USA). The chi-square test was used to analyze the relationship between CILA1 and p-β-catenin level and the clinicopathological characteristics. Spearman correlations were used to measure the association between variables. A log-rank test was performed to draw Kaplan-Meier survival curves. All experiments with cell cultures were performed at least in triplicate. The results are expressed as the mean ± SD, and $p < 0.05$ was considered statistically significant.

Accession Number

The accession number for the array data reported in this paper is GEO: GSE111585.

SUPPLEMENTAL INFORMATION

Supplemental Information includes five figures and three tables and can be found with this article online at https://doi.org/10.1016/j.ymthe.2018.04.002.

AUTHOR CONTRIBUTIONS

Zhaoyu Lin, Lijuan Sun, Shule Xie, Shanyi Zhang and Song Fan performed the in vitro assays; Qunxing Li, Weixiong Chen, and Guokai Pan performed in vivo experiments; Weiwei Wang, Zhang Zhang and Bin Weng collected and analyzed the data; Zhaoyu Lin wrote the manuscript; Bodu Liu and Jinsong Li designed the study. All authors read and approved the final manuscript.

CONFLICTS OF INTEREST

The authors have no conflicts of interest to declare.

ACKNOWLEDGMENTS

This work was supported by the National Natural Science Foundation of China (grants 81672676, 81472521, and 81272951 to J.L. and grant 81602379 to Z.L.), the Guangdong Provincial Natural Science Foundation (grant 2017A030311011 to J.L.), the Specialized Research Fund for the Doctoral Program of Higher Education (grant 20110171110068 to J.L.), the Science and Technology Project of Guangzhou City (grant 2012J4100078 to J.L.), the China Postdoctoral Science Foundation (grant 2016M590839 to Z.L.), the Fundamental Research Funds for the Central Universities (grant 13ykpy27 to L.S.), the Fund for Excellent Doctoral Dissertation of Guangdong Province (grant SYBZZXM201304 to L.S.), the Key Laboratory of Malignant Tumor Molecular Mechanism and Translational Medicine of Guangzhou Bureau of Science and Information Technology (grant [2013]163), and the Key Laboratory of Malignant Tumor Gene Regulation and Target Therapy of Guangdong Higher Education Institutes (grant K1809001).

REFERENCES

1. Chung, M.K., Min, J.Y., So, Y.K., Ko, Y.H., Jeong, H.S., Son, Y.I., and Baek, C.H. (2010). Correlation between lymphatic vessel density and regional metastasis in squamous cell carcinoma of the tongue. Head Neck *32*, 445–451.
2. Hasegawa, T., Shibuya, Y., Takeda, D., Iwata, E., Saito, I., Kakei, Y., Sakakibara, A., Akashi, M., Minamikawa, T., and Komori, T. (2017). Prognosis of oral squamous cell carcinoma patients with level IV/V metastasis: an observational study. J. Craniomaxillofac. Surg. *45*, 145–149.
3. Sano, D., and Myers, J.N. (2007). Metastasis of squamous cell carcinoma of the oral tongue. Cancer Metastasis Rev. *26*, 645–662.
4. Wu, G., Wilson, G., George, J., Liddle, C., Hebbard, L., and Qiao, L. (2017). Overcoming treatment resistance in cancer: current understanding and tactics. Cancer Lett. *387*, 69–76.
5. Zhong, L.P., Zhang, C.P., Ren, G.X., Guo, W., William, W.N., Jr., Sun, J., Zhu, H.G., Tu, W.Y., Li, J., Cai, Y.L., et al. (2013). Randomized phase III trial of induction chemotherapy with docetaxel, cisplatin, and fluorouracil followed by surgery versus up-front surgery in locally advanced resectable oral squamous cell carcinoma. J. Clin. Oncol. *31*, 744–751.
6. Gibson, M.K., Li, Y., Murphy, B., Hussain, M.H., DeConti, R.C., Ensley, J., and Forastiere, A.A.; Eastern Cooperative Oncology Group (2005). Randomized phase III evaluation of cisplatin plus fluorouracil versus cisplatin plus paclitaxel in advanced head and neck cancer (E1395): an intergroup trial of the Eastern Cooperative Oncology Group. J. Clin. Oncol. *23*, 3562–3567.
7. Sun, L., Yao, Y., Liu, B., Lin, Z., Lin, L., Yang, M., Zhang, W., Chen, W., Pan, C., Liu, Q., et al. (2012). MiR-200b and miR-15b regulate chemotherapy-induced epithelial-mesenchymal transition in human tongue cancer cells by targeting BMI1. Oncogene *31*, 432–445.
8. Thiery, J.P., Acloque, H., Huang, R.Y., and Nieto, M.A. (2009). Epithelial-mesenchymal transitions in development and disease. Cell *139*, 871–890.
9. Nieto, M.A., Huang, R.Y., Jackson, R.A., and Thiery, J.P. (2016). EMT: 2016. Cell *166*, 21–45.
10. Zhang, P.F., Li, K.S., Shen, Y.H., Gao, P.T., Dong, Z.R., Cai, J.B., Zhang, C., Huang, X.Y., Tian, M.X., Hu, Z.Q., et al. (2016). Galectin-1 induces hepatocellular carcinoma EMT and sorafenib resistance by activating FAK/PI3K/AKT signaling. Cell Death Dis. *7*, e2201.
11. Yu, F., Li, G., Gao, J., Sun, Y., Liu, P., Gao, H., Li, P., Lei, T., Chen, Y., Cheng, Y., et al. (2016). SPOCK1 is upregulated in recurrent glioblastoma and contributes to metastasis and Temozolomide resistance. Cell Prolif. *49*, 195–206.
12. Gu, P., Chen, X., Xie, R., Han, J., Xie, W., Wang, B., Dong, W., Chen, C., Yang, M., Jiang, J., et al. (2017). lncRNA HOXD-AS1 regulates proliferation and chemo-resistance of castration-resistant prostate cancer via recruiting WDR5. Mol. Ther. *25*, 1959–1973.
13. Xu, T.P., Liu, X.X., Xia, R., Yin, L., Kong, R., Chen, W.M., Huang, M.D., and Shu, Y.Q. (2015). SP1-induced upregulation of the long noncoding RNA TINCR regulates cell proliferation and apoptosis by affecting KLF2 mRNA stability in gastric cancer. Oncogene *34*, 5648–5661.
14. Özeş, A.R., Miller, D.F., Özeş, O.N., Fang, F., Liu, Y., Matei, D., Huang, T., and Nephew, K.P. (2016). NF-κB-HOTAIR axis links DNA damage response, chemoresistance and cellular senescence in ovarian cancer. Oncogene *35*, 5350–5361.
15. Kong, J., Sun, W., Li, C., Wan, L., Wang, S., Wu, Y., Xu, E., Zhang, H., and Lai, M. (2016). Long non-coding RNA LINC01133 inhibits epithelial-mesenchymal transition and metastasis in colorectal cancer by interacting with SRSF6. Cancer Lett. *380*, 476–484.
16. Liu, B., Sun, L., Liu, Q., Gong, C., Yao, Y., Lv, X., Lin, L., Yao, H., Su, F., Li, D., et al. (2015). A cytoplasmic NF-κB interacting long noncoding RNA blocks IκB phosphorylation and suppresses breast cancer metastasis. Cancer Cell *27*, 370–381.
17. Lin, Z., Sun, L., Chen, W., Liu, B., Wang, Y., Fan, S., Li, Y., and Li, J. (2014). miR-639 regulates transforming growth factor beta-induced epithelial-mesenchymal transition in human tongue cancer cells by targeting FOXC1. Cancer Sci. *105*, 1288–1298.
18. Wang, Y., Lin, Z., Sun, L., Fan, S., Huang, Z., Zhang, D., Yang, Z., Li, J., and Chen, W. (2014). Akt/Ezrin Tyr353/NF-κB pathway regulates EGF-induced EMT and metastasis in tongue squamous cell carcinoma. Br. J. Cancer *110*, 695–705.
19. Zheng, K., Zhou, X., Yu, J., Li, Q., Wang, H., Li, M., Shao, Z., Zhang, F., Luo, Y., Shen, Z., et al. (2016). Epigenetic silencing of miR-490-3p promotes development of an aggressive colorectal cancer phenotype through activation of the Wnt/β-catenin signaling pathway. Cancer Lett. *376*, 178–187.
20. Kikuchi, A., Yamamoto, H., and Kishida, S. (2007). Multiplicity of the interactions of Wnt proteins and their receptors. Cell. Signal. *19*, 659–671.
21. Yang, K., Wang, X., Zhang, H., Wang, Z., Nan, G., Li, Y., Zhang, F., Mohammed, M.K., Haydon, R.C., Luu, H.H., et al. (2016). The evolving roles of canonical WNT signaling in stem cells and tumorigenesis: implications in targeted cancer therapies. Lab. Invest. *96*, 116–136.
22. Henry, C.E., Llamosas, E., Djordjevic, A., Hacker, N.F., and Ford, C.E. (2016). Migration and invasion is inhibited by silencing ROR1 and ROR2 in chemoresistant ovarian cancer. Oncogenesis *5*, e226.
23. Han, P., Li, J.W., Zhang, B.M., Lv, J.C., Li, Y.M., Gu, X.Y., Yu, Z.W., Jia, Y.H., Bai, X.F., Li, L., et al. (2017). The lncRNA CRNDE promotes colorectal cancer cell proliferation and chemoresistance via miR-181a-5p-mediated regulation of Wnt/β-catenin signaling. Mol. Cancer *16*, 9.
24. Li, J., Yang, S., Su, N., Wang, Y., Yu, J., Qiu, H., and He, X. (2016). Overexpression of long non-coding RNA HOTAIR leads to chemoresistance by activating the Wnt/β-catenin pathway in human ovarian cancer. Tumour Biol. *37*, 2057–2065.
25. Li, Z., Zhao, L., and Wang, Q. (2016). Overexpression of long non-coding RNA HOTTIP increases chemoresistance of osteosarcoma cell by activating the Wnt/β-catenin pathway. Am. J. Transl. Res. *8*, 2385–2393.
26. Wang, Y., He, L., Du, Y., Zhu, P., Huang, G., Luo, J., Yan, X., Ye, B., Li, C., Xia, P., et al. (2015). The long noncoding RNA lncTCF7 promotes self-renewal of human liver cancer stem cells through activation of Wnt signaling. Cell Stem Cell *16*, 413–425.
27. Wu, Z.Q., Li, X.Y., Hu, C.Y., Ford, M., Kleer, C.G., and Weiss, S.J. (2012). Canonical Wnt signaling regulates Slug activity and links epithelial-mesenchymal transition with epigenetic Breast Cancer 1, Early Onset (BRCA1) repression. Proc. Natl. Acad. Sci. USA *109*, 16654–16659.
28. Li, Y., Jin, K., van Pelt, G.W., van Dam, H., Yu, X., Mesker, W.E., Ten Dijke, P., Zhou, F., and Zhang, L. (2016). c-Myb enhances breast cancer invasion and metastasis through the Wnt/β-catenin/Axin2 pathway. Cancer Res. *76*, 3364–3375.
29. Zhao, H., Hou, W., Tao, J., Zhao, Y., Wan, G., Ma, C., and Xu, H. (2016). Upregulation of lncRNA HNF1A-AS1 promotes cell proliferation and metastasis in osteosarcoma through activation of the Wnt/β-catenin signaling pathway. Am. J. Transl. Res. *8*, 3503–3512.

30. Liu, C.C., Cai, D.L., Sun, F., Wu, Z.H., Yue, B., Zhao, S.L., Wu, X.S., Zhang, M., Zhu, X.W., Peng, Z.H., and Yan, D.W. (2017). FERMT1 mediates epithelial-mesenchymal transition to promote colon cancer metastasis via modulation of β-catenin transcriptional activity. Oncogene *36*, 1779–1792.

31. Gao, Y., Liu, Z., Zhang, X., He, J., Pan, Y., Hao, F., Xie, L., Li, Q., Qiu, X., and Wang, E. (2013). Inhibition of cytoplasmic GSK-3β increases cisplatin resistance through activation of Wnt/β-catenin signaling in A549/DDP cells. Cancer Lett. *336*, 231–239.

32. Shi, S.J., Wang, L.J., Yu, B., Li, Y.H., Jin, Y., and Bai, X.Z. (2015). LncRNA-ATB promotes trastuzumab resistance and invasion-metastasis cascade in breast cancer. Oncotarget *6*, 11652–11663.

33. Han, Y., Ye, J., Wu, D., Wu, P., Chen, Z., Chen, J., Gao, S., and Huang, J. (2014). LEIGC long non-coding RNA acts as a tumor suppressor in gastric carcinoma by inhibiting the epithelial-to-mesenchymal transition. BMC Cancer *14*, 932.

34. Mohammed, M.K., Shao, C., Wang, J., Wei, Q., Wang, X., Collier, Z., Tang, S., Liu, H., Zhang, F., Huang, J., et al. (2016). Wnt/β-catenin signaling plays an ever-expanding role in stem cell self-renewal, tumorigenesis and cancer chemoresistance. Genes Dis. *3*, 11–40.

35. Peng, C., Zhang, X., Yu, H., Wu, D., and Zheng, J. (2011). Wnt5a as a predictor in poor clinical outcome of patients and a mediator in chemoresistance of ovarian cancer. Int. J. Gynecol. Cancer *21*, 280–288.

36. Anastas, J.N., Kulikauskas, R.M., Tamir, T., Rizos, H., Long, G.V., von Euw, E.M., Yang, P.T., Chen, H.W., Haydu, L., Toroni, R.A., et al. (2014). WNT5A enhances resistance of melanoma cells to targeted BRAF inhibitors. J. Clin. Invest. *124*, 2877–2890.

37. Conti, B., Minutolo, A., Arciello, M., and Balsano, C. (2013). Are Hedgehog and Wnt/β-catenin pathways involved in hepatitis C virus-mediated EMT? J. Hepatol. *58*, 636–637.

38. Yang, S., Liu, Y., Li, M.Y., Ng, C.S.H., Yang, S.L., Wang, S., Zou, C., Dong, Y., Du, J., Long, X., et al. (2017). FOXP3 promotes tumor growth and metastasis by activating Wnt/β-catenin signaling pathway and EMT in non-small cell lung cancer. Mol. Cancer *16*, 124.

39. Cho, Y.H., Cha, P.H., Kaduwal, S., Park, J.C., Lee, S.K., Yoon, J.S., Shin, W., Kim, H., Ro, E.J., Koo, K.H., et al. (2016). KY1022, a small molecule destabilizing Ras via targeting the Wnt/β-catenin pathway, inhibits development of metastatic colorectal cancer. Oncotarget *7*, 81727–81740.

40. Tseng, J.C., Lin, C.Y., Su, L.C., Fu, H.H., Yang, S.D., and Chuu, C.P. (2016). CAPE suppresses migration and invasion of prostate cancer cells via activation of non-canonical Wnt signaling. Oncotarget *7*, 38010–38024.

YMTHE, Volume *26*

Supplemental Information

Chemotherapy-Induced Long Non-coding RNA 1 Promotes Metastasis and Chemo-Resistance of TSCC via the Wnt/β-Catenin Signaling Pathway

Zhaoyu Lin, Lijuan Sun, Shule Xie, Shanyi Zhang, Song Fan, Qunxing Li, Weixiong Chen, Guokai Pan, Weiwei Wang, Bin Weng, Zhang Zhang, Bodu Liu, and Jinsong Li

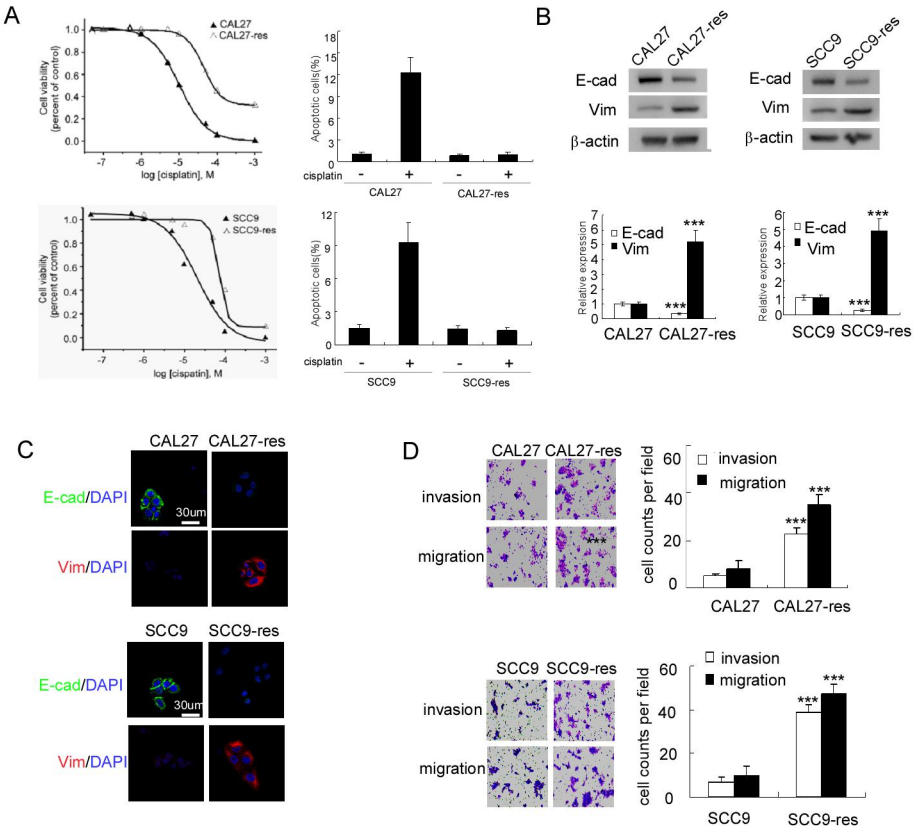

Supplementary Fig. 1. Cisplatin-resistant TSCC cells have undergone EMT. (A) MTS assay and flow cytometry were performed to assay cell viability and cell apoptosis. (B) Western blotting, qRT-PCR and (C) immunofluorescence staining illustrated reduced expression of *E-cadherin* (*E-cad*) and increased expression of *vimentin* (*Vim*) in chemoresistant TSCC cells. Nuclei: blue, scale bar: 30 μm. (D) Modified Boyden chamber assays demonstrated enhanced invasion and migration of CAL27-res and SCC9-res cells (100×).

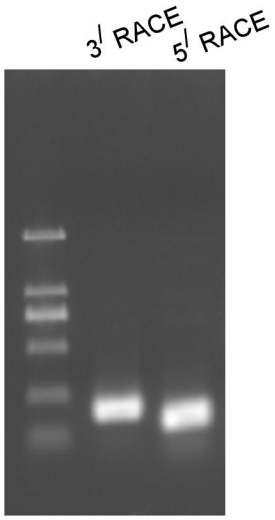

Cloned CILA1 full sequence: 709bp

TGTCTACAGCTCCCAGCTTGAGCCACGCAGAAGATGGG-
TGATTTCTGCATTTCCATCTGAGGCTACACCCTGCAAG-
GTCATTATCATTAGCTGCACTTTACAGGAGAGGAAGCT-
GAGGCTCAGAGAAGCAAACTGCCCTCCTACTTATGTTGAA
GACTTTCCCATCCTATGAGCCCAGGTGGGAGAAGCTGA-
AAATGGCAGAAGGTCACTTTTCCAGCTGCCCTGTGCCT-
GCACTTCAGGGCCAAGGAGTTTGAAGAAGTCCAAGGTA-
GAGCTTTCTGGAAAATCCTCTGGAGAGGTTGATCAGAAA
CCTTCTCCCACATAAACAAAGGACCCAGGAAGAAGCTA-
AAAATGGGCCATGAGATTGTCTTTATTCATCAAGCCTG-
AAGTTTTCTGACTCTATCTTTCTTTTCCCGTGGCCACT-
GTTACCTCTCCAGAACAGACCCCATCACCTGAATTCTGCC
TGAGCCTCGACAGATATGCTCAGCTGCTCTCCCATGCT-
GGCTGTTGTTACCCCAACCCACTTAAAATTCCTTGAG-
GTCTTAGAAGCTCTCTCCCACCAAGGTGCCGAAAGAAGT-
ATTTCACAGGTTCTCAGTGACAATTGTTTATTGAAATTTAC
ACTGATGAGAAGTGGTCCCTATTAAGGGAATTCAATC-

Supplementary Fig. 2. Full-length CILA1 was cloned and amplified by RACE.

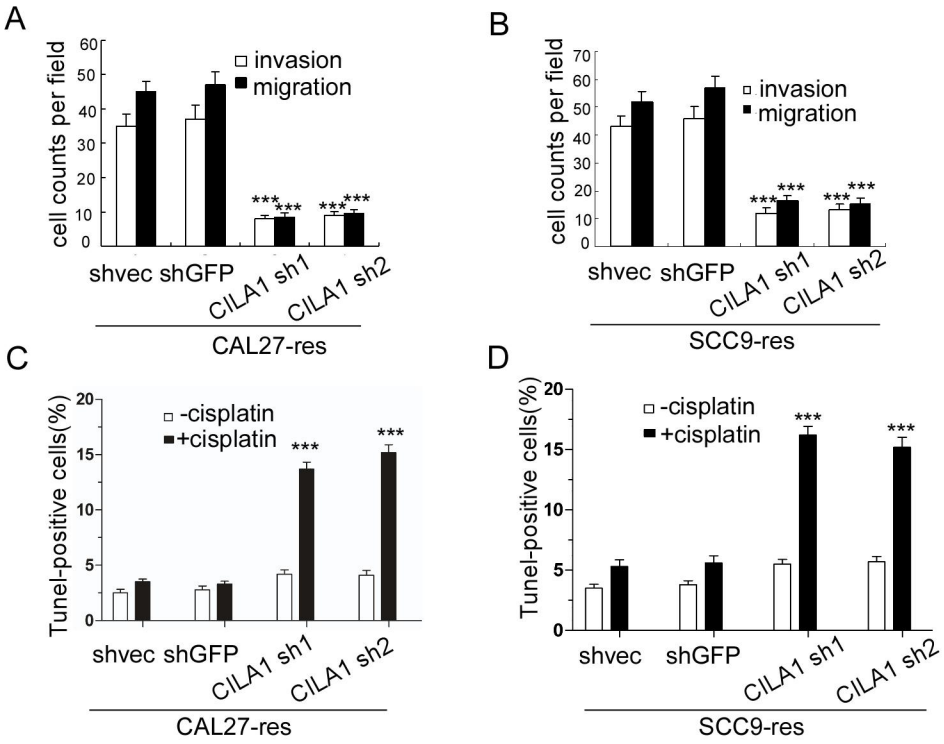

Supplementary Fig. 3. (A) and (B) Boyden chamber assays were performed to examine changes in TSCC cell motility following CILA1 downregulation. (C) and (D) TUNEL assays was performed to determine the anti-apoptotic effect following CILA1 downregulation. (***P<0.001)

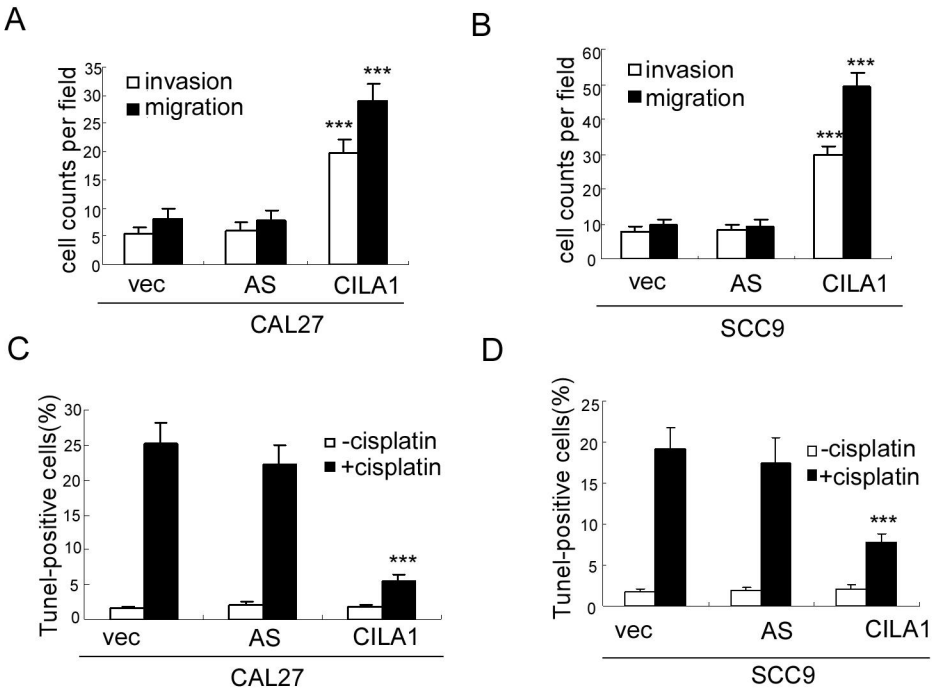

Supplementary Fig. 4. (A) and (B) Boyden chamber assays were performed to examine the changes in TSCC cell motility after upregulating CILA1 expression. (C) and (D) TUNEL assays were performed to determine the anti-apoptotic effect of CILA1 following CILA1 upregulation (***P<0.001).

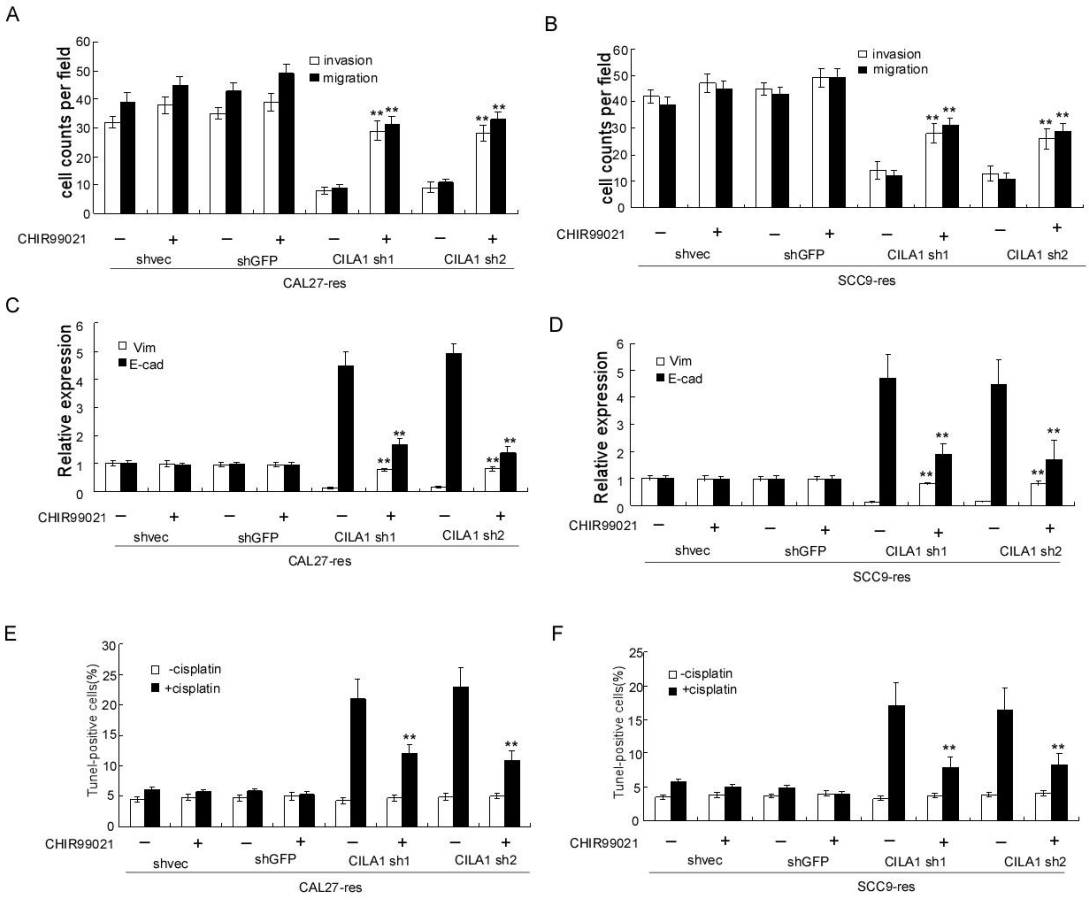

Supplementary Fig. 5. (A) and (B) Boyden chamber assays were performed to examine the effect of CHIR99021 on chemoresistant TSCC cell motility. (C) and (D) qRT-PCR was performed to examine the effect of CHIR99021 on chemoresistant TSCC cell EMT-related gene expression. (E) and (F) TUNEL assays were performed to determine the effect of CHIR99021 on chemoresistant TSCC cell apoptosis (**P<0.01).

Supplementary table 1 Fold Change(SCC9-res/SCC9) and Regulation

SEQ_ID	p-value	FCAbsolute	logFC*(-log(p-value))
ASLNC08201	0.0000151	40.070263	7.727242741
ASLNC02104	0.0000318	20.515862	5.901219362
ASLNC05042	0.000236	36.86618	5.68229812
DA720951	0.000191	28.08335	5.386733175
ASLNC18836	0.000123	21.506205	5.21045083
ASLNC07991	0.000182	20.374893	4.895923106
ASLNC16165	0.000203	20.504148	4.843980778
BE144234	0.0000182	9.462565	4.626212396
ASLNC21850	0.000257	15.9932	4.322208487
exon2743	0.001086614	23.32594	4.05417226
ASLNC06390	0.000317	12.993266	3.896834433
ASLNC23343	0.0000827	7.949204	3.67556631
CILA1	0.000729	14.196747	3.614730339
ASLNC19458	0.000068	5.5132375	3.08980582
AK124439	0.001686586	11.955446	2.988080764
ASLNC21657	0.001517045	11.404633	2.979913849
ASLNC05805	0.001378485	9.283883	2.768285483
ASLNC16838	0.000126	5.0987124	2.758833865
ASLNC12735	0.000416	6.504114	2.749313222
ASLNC16219	0.000167	5.228774	2.7136
ASLNC07749	0.000533	6.318715	2.62067636
ASLNC06008	0.001089988	7.3489647	2.566262814
exon655	0.000406	5.587273	2.534108981
AV747682	0.000337	5.026671	2.435105305
BX093190	0.002106526	7.8673916	2.397631187
ASLNC05502	0.0013531	6.6181087	2.354414792
ASLNC15926	0.000931	5.9120216	2.339170686
ASLNC01712	0.002056881	7.262441	2.313548883
ASLNC21104	0.003139346	8.216363	2.28959018
ASLNC18399	0.00182934	6.8335896	2.285022923
exon2903	0.003491177	8.311547	2.259684215
ASLNC01284	0.002171475	7.0177984	2.253640425
AK129581	0.006394999	10.48987	2.239732445
ASLNC04384	0.001681384	6.162041	2.190959044

AI744597	0.012906011	14.403054	2.188561641
ASLNC16096	0.002514039	6.338377	2.08484463
ASLNC23349	0.005283073	8.189105	2.079542923
BF873246	0.002337037	5.989154	2.045508539
ASLNC16161	0.015383688	12.371554	1.980499123
ASLNC19113	0.003221265	5.673729	1.878620579
ASLNC21416	0.003682749	5.836801	1.8647378
ASLNC01049	0.005621055	6.5286674	1.833503657
BG218484	0.007063437	6.802415	1.791044993
ASLNC09657	0.004059661	5.5203705	1.774424604
ASLNC22042	0.004811209	5.4663224	1.709790033
ASLNC24861	0.00502692	5.3837442	1.680542306
AI935368	0.042484835	16.761286	1.679463256
ASLNC15095	0.020478671	9.830807	1.676183576
ASLNC21501	0.00573784	5.3347864	1.629652194
ASLNC19961	0.009945265	6.405494	1.615027789
ASLNC19152	0.005202038	5.025704	1.601412062
ASLNC02044	0.00931661	5.991583	1.578986408
ASLNC10793	0.009341336	5.965947	1.574311916
ASLNC02958	0.006064923	5.0701323	1.563150943
ASLNC02761	0.010878156	6.21361	1.557687068
AA935188	0.013426022	6.504708	1.522405265
ASLNC01418	0.012773945	6.3594394	1.521414125
ASLNC07466	0.0256155	6.98567	1.343554741
ASLNC04559	0.022237668	5.8499594	1.268035202
exon653	0.038682684	7.7552176	1.256536741
ASLNC01177	0.022332508	5.669594	1.244161385
ASLNC09871	0.028852765	6.425439	1.244018888
ASLNC03863	0.019566856	5.1736703	1.219510138
exon654	0.032520954	6.53382	1.212835645
ASLNC06505	0.027760431	5.106413	1.102234712
ASLNC16599	0.002555202	17.212223	3.203999722

Supplementary table 2 Primers for genes involved in qRT-PCR.

Gene name		primer
bc016962	Forward	AATCTTTGCAGGTGGGCATG
	Reverse	TTGACCTGCTCATCCCAAAC
ak094950	Forward	atttgcatgctcccacgaac
	Reverse	aaccctaactccagatgtgtcg
ak001058	Forward	tggtgggtaaagcacaatcc
	Reverse	aatggcaaagcagcacagag
be144234	Forward	accaagcgagaaggaactcag
	Reverse	tcagtggcatgttggaaagc
al359062	Forward	actcggcacaaatcaaaggc
	Reverse	aggctcgaaatgggtctttg
bc042436	Forward	atgccgcaaaggtttggttg
	Reverse	atgtgtccttcccccttttcag
CILA1	Forward	tgggtgatttctgcgtttcc
	Reverse	agcttcctctcctgtaaagtgc
E-cadherin	Forward	GCCGCTGGCGTCTGTAGGAA
	Reverse	TGACCACCGCTCTCCTCCGA
β-catenin	Forward	CCAGCCGACACCAAGAAGCA
	Reverse	GCGGGACAAAGGGCAAGATT
vimentin	Forward	TGGATTCACTCCCTCTGGTTG
	Reverse	CGTGATGCTGAGAAGTTTCGTT
GAPDH	Forward	ACCCAGAAGACTGTGGATGG
	Reverse	GAGGCAGGGATGATGTTCTG

Supplementary table 3 Primary antibodies used in the study.

Antibody	MV (KDa)	Sources (Catalogue #)	Dilution
E-cadherin	135	Cell Signaling Technology (#3195) (Beverly, MA)	WB:1:2000, IF:1:200
Vimentin	57	Cell Signaling Technology (#5741) (Beverly, MA)	WB:1:2000, IF:1:100
GSK3β	46	Cell Signaling Technology (#9315) (Beverly, MA)	WB:1:1000
p-GSK3β(Ser9)	46	Cell Signaling Technology (#9336) (Beverly, MA)	WB:1:1000
β-catenin	92	Cell Signaling Technology (#8480) (Beverly, MA)	WB:1:2000,IF:1:100
p-β-catenin(Ser33/37/Thr41)	92	Cell Signaling Technology (#9561) (Beverly, MA)	WB:1:1000
c-Myc	57	Cell Signaling Technology (#9402) (Beverly, MA)	WB:1:1000
survivin	16	Santa cruz(#sc-D8) (California)	WB:1:200
Lamin B1	68	Cell Signaling Technology (#13435) (Beverly, MA)	WB:1:1000
PCNA	36	Cell Signaling Technology (#2586) (Beverly, MA)	IHC: 1:4000
GAPDH	36	Proteintech,(#10494) (Chicago, IL)	WB:1:5000
β-actin	45	Cell Signaling Technology (#3700) (Beverly, MA)	WB:1:1000